Modeling Solubilities of Additives in Polymer Microstructures: Single-Step Perturbation Method Based on a Soft-Cavity Reference State

Tugba A. Özal, Christine Peter, Berk Hess, and Nico F. A. van der Vegt*

Max Planck Institute for Polymer Research, Ackermannweg 10, D-55128 Mainz, Germany

Received October 19, 2007; Revised Manuscript Received April 4, 2008

ABSTRACT: Solubilities of additive molecules whose molecular sizes exceed the typical dimensions of free volume cavities pre-existing in amorphous polymer melts and glasses cannot readily be computed in molecular simulations. In this paper, we perform molecular dynamics simulations of a soft-cavity reference state ensemble, which contains a soft-core, fast diffusing, Lennard-Jones particle in a rigid-chain polymer matrix. By means of the Zwanzig thermodynamic perturbation formalism, the soft particle has been perturbed to various real-solute end-states. It is shown that with this approach it is possible to overcome some of the free energy sampling problems related to the insertion of large solutes and slow diffusion in the end-state. We have calculated the excess chemical potentials of propane, chloroform, and dimethyl sulfoxide in liquid bisphenol A−polycarbonate and show that a single simulation of the reference state is sufficient to obtain statistical accuracies within error bars of 0.5−0.8 k_BT. The method is particularly useful for calculating solubility ratios of large molecular solutes with approximately equal excluded volume radii.

1. Introduction

Chemical potentials of solute molecules dissolved in dense polymer microstructures can in principle be calculated using molecular simulation methods.[1] In particular, the test-particle-insertion method by Widom[2] has frequently been applied to gas molecules[3–11] because these solutes are typically small (diameters smaller than ∼4 Å) and can readily be inserted in empty cavities pre-existing in all amorphous polymer microstructures. The case is different for larger solutes. These solutes, which are at ambient temperatures usually in a liquid or vapor phase, represent a substantially larger perturbation and, unlike in the Widom particle insertion method, usually cannot be inserted "at once". Widom insertion methods combined with excluded volume map sampling (EVMS)[12] and/or configurational bias Monte Carlo (CBMC)[13] sampling have been used to compute chemical potentials of larger solutes in polymer microstructures.[6,8,14–16] Even though CBMC has proven to work very well for flexible solutes (e.g., alkanes) in low-T_G (rubbery) polymer matrices, both EVMS and CBMC insertion-based methods fail in case the reference ensemble (polymer matrix) does not sample cavity spaces of appropriate size needed for solute insertion during a finite length simulation.

Alternatively, one can resort to methods in which the solute coupling with the polymer microstructure is introduced in small steps, thus allowing the solute to create its required cavity space and the chain environment to locally adjust to the solute. Thermodynamic coupling parameter integration[17] (TI) is a commonly used technique that can be employed for this purpose. Although TI is seemingly more suitable for larger solutes in rigid polymers, it lacks the advantage of insertion-based methods where volume averaging over the microstructure is achieved by performing insertions at many randomly chosen locations. This becomes particularly problematic in molecular dynamics (MD) simulations of (slow diffusing) polymeric systems where the solute particle, on time scales of nanoseconds, stays trapped inside a local cavity and explores only very small distance scales. To obtain statistically meaningful results, several independent TI calculations need then to be performed with independently coupled particles exploring different cavities. This can be done using fast-growth TI[18] and employing Jarzynski's equality[19] for the free energy change, as has recently been discussed elsewhere.[20] Note that in systems where the solute is present at finite concentration the same approach of perturbing only one solute should still be followed rather than coupling (or decoupling) all solutes at once since the latter approach would provide the excess chemical potential averaged over the entire concentration window. Knopp et al.,[21] in their study of water solubility in polymers, nevertheless used this approach however only to the attractive part of the water−polymer and water−water nonbonded interaction potential which may be justified if the corresponding contribution to the free energy change depends only weakly on solute concentration. In another approach,[22] the problem of coupled particles getting trapped and exploring only small distance scales could be resolved using extended ensemble molecular dynamics (EEMD) simulations. In EEMD the parameter that couples the test particle to the rest of the system is treated as a dynamic variable. Although this method turned out to be superior in comparison to (slow-growth) TI, it requires an a priori unknown umbrella potential that eliminates free energy barriers that may exist at various values of the coupling parameter.

In this paper we propose an alternative technique that combines the advantages of the thermodynamic integration and particle insertion methods. It is based on earlier ideas[23–27] in which carefully designed stages are introduced in free energy perturbation calculations. In refs 26 and 27, a particle deletion method has been described introducing an intermediate stage in the calculation where the solute particle to be removed was substituted by a hard particle. On the basis of Monte Carlo simulations, excess chemical potentials of Lennard-Jones fluids could successfully be calculated using a fast analytical algorithm for the computation of the volume accessible to the hard-core particle.[26] This method has subsequently been extended to chain molecules[27] and has been implemented in molecular dynamics simulations of small gaseous solutes and benzene in poly(dimethylsiloxane).[28] In chemically complex polymers, a large hard-sphere intermediate may not be an optimal stage. Because the hard-sphere accessible space needs to be calculated on the basis of molecular simulations of the reference ensemble, the success

* Corresponding author. E-mail: vdervegt@mpip-mainz.mpg.de.

10.1021/ma702329q CCC: $40.75
Published on Web 06/03/2008

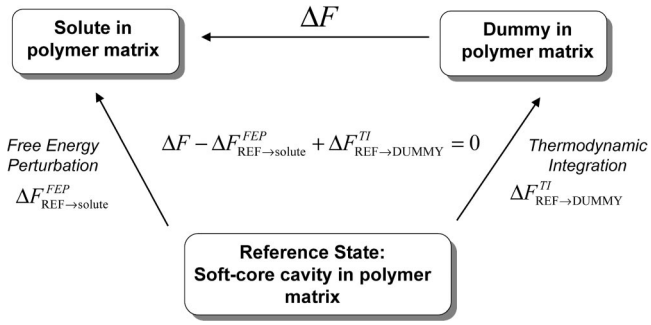

Figure 1. Thermodynamic cycle for calculating the free energy change of solvation (ΔF).

of the method relies on the question of whether this volume is sampled, which, as discussed above, may be problematic. In this paper we propose to introduce a *soft-cavity* reference state,[29] which is defined by the polymeric microstructure in which a soft-core Lennard-Jones particle has been introduced. By virtue of its optimized softness, this particle explores the simulated volume on time scales of nanoseconds while at the same time creating the space requirements for insertion of large and rigid solutes. The free energy of the target state relative to the soft intermediate state is obtained by free energy perturbation[30] (FEP) calculations, while the free energy of the soft intermediate state, relative to the system excluding the soft-core particle, can straightforwardly be obtained with TI (see Figure 1). The latter (TI) calculation is accurate because the soft-particle—unlike real molecules with hard-core repulsions—does not get trapped locally. In this paper we test the applicability of this method in liquid octadecane as well as in a bisphenol A−polycarbonate (BPA−PC) microstructure.

2. Methods

Before we introduce the general concept of the method used in this work, we briefly summarize some aspects of the TI and FEP methods used in this paper.

2.1. TI and FEP. *Thermodynamic Integration (TI).* The TI expression for the Helmholtz free energy change of introducing nonbonded interactions between a solute molecule (the "coupled" solute), and the remainder of the system reads[17]

$$\Delta F^{\mathrm{TI}} = \int_0^1 \left\langle \frac{\partial V_{\mathrm{SC}}(\lambda)}{\partial \lambda} \right\rangle_\lambda \mathrm{d}\lambda \tag{1}$$

where

$$V_{\mathrm{SC}}(\lambda) = (1-\lambda)\sum_{i,j} V_{ij}(r_{\mathrm{SC}}(r_{ij};\lambda))$$

with

$$r_{\mathrm{SC}}(r_{ij};\lambda) = \left(\alpha\sigma_{ij}{}^6\lambda + r_{ij}{}^6\right)^{1/6} \tag{2}$$

In eq 1, $\langle ... \rangle_\lambda$ denotes an average over a canonical ensemble of states sampled with Hamiltonian $\mathbf{H}(\lambda)$; the dependence on the coupling parameter λ results from the coupled solute−system potential energy described by the soft-core (SC) potential $V_{\mathrm{SC}}(\lambda)$. The coupling parameter values $\lambda = 0$ and $\lambda = 1$ correspond to the fully coupled and uncoupled states, respectively. In eq 2, $V_{ij}(r)$ is the site−site pair potential, which includes Lennard-Jones (LJ) and, in case of polar solutes with partial atomic charges, Coulomb terms. In case of a single solute in a polymer matrix, the sum in eq 2 runs over all pairs ij that correspond to having one interaction site located on the coupled solute and another located on the polymer. At finite solute concentrations, the sum in eq 2 also runs over pairs ij corresponding to interaction sites on the coupled solute and all other solutes. In eq 2, σ_{ij} and r_{ij} are the LJ size parameter and interparticle distance of the atom pair ij, respectively. In our calculations, we used a soft-core parameter $\alpha = 0.7$. Because the integration process always involves the coupling of only one solute molecule with the remainder of the system, eq 1 provides the solute excess chemical potential at the corresponding solute concentration, i.e., $\Delta F^{\mathrm{TI}} = \mu_{\mathrm{ex}}$. Note that in case of nonrigid (internally flexible) solutes the calculated excess chemical potential includes contributions arising from changes in the way the solute internal degrees of freedom are modified by the polymer.

We note that the thermodynamic integration process of introducing nonbonded interactions (eq 1) is equivalent to the process of transferring a solute molecule from a fixed position in the ideal gas phase to a fixed position in the polymer phase and, therefore, is directly related to the ideal gas phase solubility of the respective solute. The relation between μ_{ex} and the ideal gas phase solubility, S, with commonly reported units cm^3 (STP)/cm^3 , is given by[10] $S = (T_0/P_0T)\exp(-\mu_{\mathrm{ex}}/RT)$, where T_0, P_0, R, and T are the standard temperature (273.15 K), standard pressure (1 atm), gas constant, and the absolute temperature, respectively.

Free Energy Perturbation (FEP). The free energy perturbation formula for the Helmholtz free energy difference between two systems A and B is given by[30]

$$\Delta F^{\mathrm{FEP}}_{\mathrm{A}\rightarrow\mathrm{B}} = F_{\mathrm{B}} - F_{\mathrm{A}} = -k_{\mathrm{B}}T\ln\langle \mathrm{e}^{-\beta(U_{\mathrm{B}}-U_{\mathrm{A}})}\rangle_{\mathrm{A}} \tag{3}$$

where $\beta = 1/k_{\mathrm{B}}T$, with k_{B} Boltzmann's constant and T the absolute temperature, and U is the configurational energy with subscripts A and B referring to the two systems of interest. The angular brackets indicate a canonical (NVT) ensemble average performed on the A system which we call the reference (the B system is the target).[25] In the calculation of an excess chemical potential by one-step FEP, the A system represents the polymer matrix containing N_{S} solutes and the B system represents the polymer matrix containing $N_{\mathrm{S}} + 1$ solutes. In this paper we shall be concerned with the case $N_{\mathrm{S}} = 0$.

2.2. FEP and TI Using a Soft-Cavity Reference State. *General Concept.* Figure 1 shows a thermodynamic cycle summarizing the approach examined in this work. The horizontal arrow represents the process of introducing nonbonded interactions between the solute molecule and the polymeric microstructure. The solute excess chemical potential amounts to the free energy difference ΔF between the two states connected by this process. TI or FEP can in principle be used to compute this quantity, but in practice they face severe sampling problems in slow diffusing systems with large-sized solutes. As was mentioned before, TI suffers from poor sampling over the volume of the amorphous microstructure (diffusion problem); FEP suffers from insertion problems usually encountered in dense systems. TI and FEP can however be combined in a way that alleviates the sampling problems encountered in both methods. The idea is to introduce a "soft" intermediate (reference) state[23–26,29] (Figure 1) corresponding to a soft-core Lennard-Jones particle (defined by eq 2) embedded in the matrix. Because diffusion barriers for the motions of the soft-core particle are small, the box volume and relevant cavity spaces can be sampled in a short MD run. The chemical potentials of the solute (Figure 1, upper left corner) and noninteracting dummy particle (upper right corner)—relative to the soft-core reference—can readily be obtained by FEP and TI, respectively. In the FEP step (cf. eq 3) from SC to solute, the soft-core reference ensemble (REF) is used, and the perturbation energy $\Delta U = U_{\mathrm{solute}} - U_{\mathrm{REF}}$ is defined as the potential energy U_{solute} of the system with the real solute (located at the position of the soft particle) relative to the potential energy U_{REF} of the soft-cavity reference system. In the TI step from SC to dummy, the soft-core particle is gradually changed into

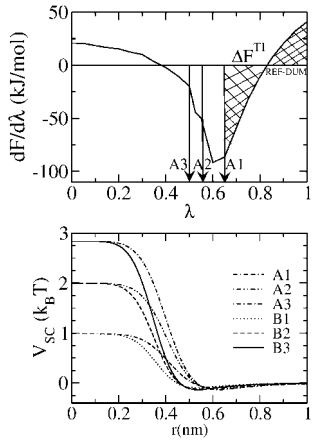

Figure 2. (upper panel) Free energy (TI) curve of Lennard-Jones particle A (see Table 1) in liquid octadecane (1 ns equilibration and 1 ns production per λ-point). The shaded area represents $\Delta F^{\mathrm{TI}}_{\mathrm{REF}\rightarrow\mathrm{DUMMY}}$ for reference soft core particle A1. Reference states A1, A2, and A3 are indicated with arrows. (lower panel) Soft-core potential energy functions $V_{\mathrm{SC}}(r,\lambda)$ of some chosen reference states (see Table 1) with octadecane methylene groups at 323 K. The A and B reference states differ with respect to the soft-core size parameters, which are $\sigma_{\mathrm{SC}} = 0.8$ and 0.6 nm for the A and B states, respectively.

a dummy particle. Both the FEP and the TI steps do not suffer from inadequately sampling the volume of the simulation cell. Because the free energy change of the closed cycle is zero, the excess chemical potential is obtained from the difference between FEP and TI free energies relative to the reference state.

Choice of the Reference State. The above concept introduces an optimization problem that we briefly discuss here and treat in greater detail later on. On the one hand the soft-core reference must to some extent retain the hard-core repulsive nature of the intermolecular potential of any real solute in order to keep the perturbation energy ΔU small (cavities are then produced into which the solute fits). Only then, the configurational spaces of the final and reference systems have sufficient overlap and the traditional insertion problem can be circumvented. The soft-core particle must on the other hand be significantly softer than real solutes in order to sample the overall system volume and the potential cavity spaces in the microstructure efficiently.

We model the soft reference ensemble by running an MD simulation of a softened LJ particle in the polymeric microstructure. The size and softness of this particle are determined through the choice of the parameters λ, α, σ, and ε in eq 2. The LJ size and energy parameters σ and ε depend on the atom pair considered and are defined as $\sigma = (\sigma_{\mathrm{SC}}\sigma_{\mathrm{atom}}^{\mathrm{matrix}})^{1/2}$ and $\varepsilon = (\varepsilon_{\mathrm{SC}}\varepsilon_{\mathrm{atom}}^{\mathrm{matrix}})^{1/2}$ for the octadecane systems. Lorentz−Berthelot combination rules ($\sigma = (\sigma_{\mathrm{SC}} + \sigma_{\mathrm{atom}}^{\mathrm{matrix}})/2$ and $\varepsilon = (\varepsilon_{\mathrm{SC}}\varepsilon_{\mathrm{atom}}^{\mathrm{matrix}})^{1/2}$) have been used for BPA−PC to be consistent with the BPA−PC force field.[31] Because α (=0.7) is kept fixed, the softness is determined by the choice of λ (we refer to this choice as λ^*), which is made based on two criteria: (i) the soft-core pair potential with any of the matrix atoms at full overlap ($r = 0$) should be of the order of the thermal energy $k_{\mathrm{B}}T$ and (ii) $\partial\Delta F/\partial\lambda = \langle\partial U_{\mathrm{SC}}/\partial\lambda\rangle$ in the interval $\lambda \in [\lambda^*,1]$ must be a precisely sampled, ideally monotonic function of λ because that permits using TI to calculate $\Delta F^{\mathrm{TI}}_{\mathrm{REF}\rightarrow\mathrm{DUMMY}}$ (see Figure 1) with high accuracy.

Figure 2 (upper panel) shows a "TI curve" ($\partial\Delta F/\partial\lambda$ vs λ) corresponding to a LJ particle (corresponding to reference state A in Table 1) in liquid octadecane. Arrows are included at three values of λ, and the corresponding soft-core potentials are shown in the lower panel. The maximum values of the potentials (at $r = 0$) are $k_{\mathrm{B}}T$, $2k_{\mathrm{B}}T$, and $3k_{\mathrm{B}}T$ for potentials A1, A2, and A3, respectively (Figure 2, lower panel). Although it is clear that $\Delta F^{\mathrm{TI}}_{\mathrm{REF}\rightarrow\mathrm{DUMMY}}$ will be obtained most accurately with soft-core reference state A1, it is unclear whether the corresponding, small barrier height is sufficient to successfully perform the FEP calculation. For this reason three choices are taken for the soft-core reference.

Table 1. Parameters for the Reference State Lennard-Jones Particles (Eq 2)[a]

system	reference	λ	$V_{\mathrm{SC}}(r=0,\lambda)$ (kJ/mol)	$\varepsilon_{\mathrm{SC}}$ (kJ/mol)	σ_{SC} (nm)
octadecane	A1	0.65	2.6	1.2532	0.8
	A2	0.55	5.4		
	A3	0.50	7.6		
	B1	0.65	2.6	1.2532	0.6
	B2	0.55	5.4		
	B3	0.50	7.6		
BPA−PC	C2	0.60	3.2 (5.0)	1.2532	0.8
	C3	0.55	4.5 (7.1)		
	C4	0.45	9.2 (14.4)		
	D2	0.65	2.2 (3.5)	1.2532	0.7
	D3	0.60	3.2 (5.0)		

[a] The A and B references apply to octadecane, and the C and D references apply to BPA-PC. $V_{\mathrm{SC}}(r=0,\lambda)$ denotes the maximum of the soft particle−matrix atom potential at full particle overlap. For octadecane $V_{\mathrm{SC}}(r=0,\lambda)$ refers to CH_2 units; for BPA−PC, the aromatic carbons are chosen (the values in parentheses denote the maximum soft particle interaction with carbonyl oxygens).

The parameters describing the soft-core Lennard Jones reference states are summarized in Table 1. The "A" and "B" reference states are used for the liquid octadecane systems, and the "C" and "D" reference states are used for BPA−PC.

3. Simulation Details

MD simulations of liquid octadecane were performed with a system containing 200 molecules in a periodic cubic box. The temperature was set at 323 K (corresponding $k_{\mathrm{B}}T = 2.7$ kJ/mol). The GROMOS 45A3 united atom potential was applied.[33] After including the soft Lennard-Jones particles, all systems were equilibrated for 2 ns followed by 10 ns runs for sampling the soft-cavity reference ensembles. To calculate $\Delta F^{\mathrm{FEP}}_{\mathrm{REF}\rightarrow\mathrm{SOLUTE}}$ (see Figure 1), a total of 10^5 insertions of the solutes propane, chloroform, and DMSO were performed in each snapshot of the soft-core reference trajectory stored every 1 ps. Propane, chloroform, and DMSO were described with the force fields reported in refs 33− 35. Solutes were inserted with random orientations, allowing their center of mass positions to fall within a radius of 0.05 nm from the center of the soft cavity. Slow growth TI (eq 1) was used to calculate the excess chemical potentials of the solutes in octadecane. At each λ-point, 1 ns equilibration and 1 ns sampling were performed. In total, 22 λ-points were used equally divided between 0 and 1.

In addition to octadecane, a polymer matrix of BPA−PC was simulated. BPA−PC simulations were performed at 480 K ($k_{\mathrm{B}}T = 4.0$ kJ/mol). The pressure was 1 atm in all simulations. The BPA−PC simulation box[32] contained 50 chains of five monomeric repeat units, corresponding to a total number of 9550 atoms. Note that although these chains are relatively short, the free energy sampling problems discussed in the Introduction are just as severe in this system as in microstructures composed of longer chains. Force field parameters of the BPA-PC all-atom model were taken from ref 31. For BPA-PC the simulations were performed with twin-range 0.9/1.4 nm reaction-field electrostatics. The bond lengths in the matrix as well as the internal geometries of the additives were kept constant by the SHAKE algorithm.[36] For the Lennard-Jones interaction a twin-range 0.9/1.4 nm and 1.0/1.4 nm were used for BPA−PC and octadecane, respectively. To obtain a canonical distribution when the additive is nearly decoupled from the polymer matrix, a local thermostat is required. We chose to use a Langevin

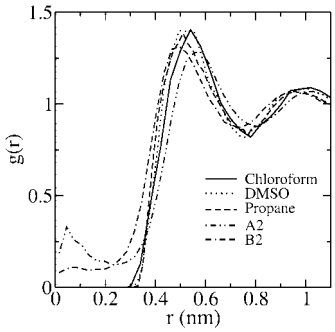

Figure 3. Radial distribution functions $g(r)$ of octadecane methylene units with chloroform carbon atom, DMSO sulfur atom, propane central carbon atom, soft-core cavity A2, and soft-core cavity B2.

thermostat with a friction coefficient of 1 ps^{-1}. A Berendsen barostat[37] was used with a coupling time of 5 ps. All simulations were performed by the GROMACS software package,[38] and for the FEP calculations a modified version of the package was used with a modification of the particle insertion routine.

4. Results and Discussion

The single-step perturbation method described in section 2 has been applied to octadecane and bisphenol A−polycarbonate. In all systems, the excess chemical potentials of propane, chloroform, and dimethyl sulfoxide have been calculated. Because a single TI run for each of the above solutes provides the excess chemical potential with sufficiently high accuracy in liquid octadecane, this system was chosen as a benchmark for optimizing the parameters characterizing the soft reference state.

Octadecane. Figure 3 shows the solute−solvent radial distribution functions (RDFs) of the target molecules propane, chloroform, and DMSO together with the soft cavity−solvent radial distribution functions in octadecane. The soft-cavity size parameter σ fixes the location of the first maximum of the soft cavity−solvent RDF, while the potential maximum $V_{SC}(r = 0)$ determines the value of the RDF at $r = 0$. While with reference A2 (see Table 1) the location of the first maximum is at slightly larger distance than the three solutes, with reference B2 the location of the first maximum is at slightly smaller distance. The overall match between the locations of the first maxima of the solutes and soft particles is however reasonably good, based on which we decided to use $\sigma = 0.6$ nm and $\sigma = 0.8$ nm for the soft-core reference potentials in octadecane (see Table 1).

The free energies of propane, chloroform, and dimethyl sulfoxide in octadecane obtained by single-step FEP with the various soft reference states are summarized in Table 2. Free energies obtained by TI are included in the last column. The soft cavity FEP data presented for the three solutes are based on a single 10 ns MD run of the soft reference state. The free energies obtained by TI in the last column of Table 2, however, required 44 ns of simulation time for each of the three solutes. Also, when taking into account equilibration times and the calculation of the remaining TI contribution $\Delta F^{TI}_{REF\rightarrow DUMMY}$ (see Figure 1), the soft cavity FEP method saves considerable computer time in comparison to performing normal TI. The soft reference FEP free energies ($\Delta F^{FEP} = \Delta F^{FEP}_{REF\rightarrow solute} - \Delta F^{TI}_{REF\rightarrow DUMMY}$) and TI free energies ($\Delta F^{TI}$) are in good agreement irrespective of the soft cavity reference state. To investigate the accuracy of the FEP step ($\Delta F^{FEP}_{REF\rightarrow solute}$), we present in Figure 4a the perturbation energy distribution $\rho(\Delta U_{REF\rightarrow DMSO})$. The energies $\Delta U_{REF\rightarrow DMSO}$ have been Boltzmann weighted over all DMSO insertion attempts per simulation snapshot of the soft reference trajectory before accumulating the histogram. In Figure 4b the quantity $\rho(\Delta U_{REF\rightarrow DMSO})$ $\exp[-\beta\Delta U_{REF\rightarrow DMSO}]$ is presented. This quantity must be sampled well over the maximum down to low energies in order to obtain an accurate estimate of the free energy $\Delta F^{FEP}_{REF\rightarrow DMSO}$, which corresponds to the integral over this reweighted distribution.[39] Comparison of parts a and b of Figure 4 illustrates the importance of sampling the low-energy tail of $\rho(\Delta U_{REF\rightarrow DMSO})$.

Table 2. Free Energy Changes (kJ/mol) in Liquid Octadecane Obtained by FEP and TI Based on a 10 ns Reference State Simulation (FEP) and 1 ns Simulations at Each λ-Point (TI)[a]

soft-cavity reference	$\Delta F^{FEP}_{REF\rightarrow SOLUTE}$	$\Delta F^{TI}_{REF\rightarrow DUMMY}$	ΔF^{FEP}	ΔF^{TI} (slow growth)
		chloroform		
A1	−16.0 (0.3)	−3.2 (0.3)	−12.8	−14.5 (1.1)
A2	−25.1 (0.2)	−11.2 (0.9)	−13.9	
A3	−27.2 (0.3)	−13.2 (1.1)	−14.0	
B1	−14.3 (0.5)	−1.7 (0.2)	−12.6	
B2	−20.6 (0.4)	−6.4 (0.6)	−14.2	
B3	−22.7 (0.4)	−7.8 (0.7)	−14.9	
		DMSO		
A1	−18.9 (0.4)	−3.2 (0.3)	−15.6	−16.9 (1.0)
A2	−27.4 (0.2)	−11.2 (0.9)	−16.1	
A3	−29.8 (0.3)	−13.2 (1.1)	−16.6	
B1	−17.3 (0.5)	−1.7 (0.2)	−15.6	
B2	−23.2 (0.5)	−6.4 (0.6)	−16.8	
B3	−25.2 (0.4)	−7.8 (0.7)	−17.4	
		propane		
A1	−8.2 (0.4)	−3.2 (0.3)	−4.9	−6.0 (0.9)
A2	−16.8 (0.2)	−11.2 (0.9)	−5.6	
A3	−19.2 (0.3)	−13.2 (1.1)	−6.0	
B1	−6.3 (0.4)	−1.7 (0.2)	−4.6	
B2	−12.4 (0.4)	−6.4 (0.6)	−6.0	
B3	−14.8 (0.5)	−7.8 (0.7)	−6.9	

[a] Errors (obtained by block averaging) are given in parentheses.

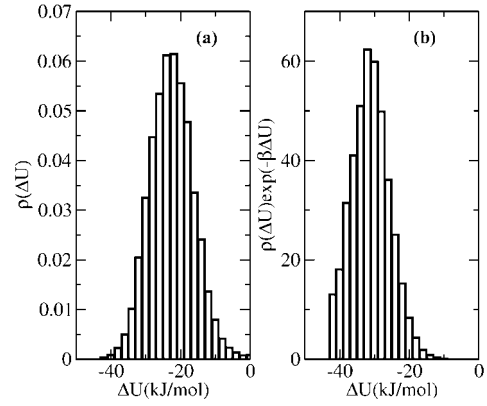

Figure 4. (a) Probability distribution function $\rho(\Delta U)$ and (b) its exponentially weighted distribution $\rho(\Delta U)\exp(-\beta\Delta U)$ corresponding to free energy perturbation of the A3 reference state to DMSO in octadecane.

Bisphenol A−Polycarbonate. The same methodology has been applied to a melt of 50 BPA-PC 5-mers at $T = 480$ K. The chemical structure of BPA−PC includes polar units (carbonate) as well as nonpolar units (isopropylidene), and therefore the solute interactions with the polymer backbone include van der Waals as well as electrostatic contributions, potentially resulting in much greater differences in the free energies of propane (nonpolar), chloroform (slightly polar), and DMSO (highly polar). In contrast to the octadecane system, slow-growth TI calculations of solute free energies in BPA−PC produced unreliable data. For example, we performed two TI calculations (23 λ-points, 1 ns sampling per λ-point) decoupling chloroform from the BPA−PC matrix starting off with the chloroform molecule at two different initial locations in the matrix. The resulting free energies were 11.9 and 5.5 kJ/mol. Similar differences were obtained with DMSO and propane.

Table 3. Free Energy Changes (kJ/mol) in BPA−PC by FEP and TI, Based on a 10 ns Reference State Simulation (FEP) and 1 ns Simulations at Each λ-Point (TI)[a]

polymer	reference	$\Delta F^{FEP}_{REF\rightarrow SOLUTE}$	$\Delta F^{TI}_{REF\rightarrow DUMMY}$	ΔF^{FEP}	ΔF^{TI} (fast growth)[20]
		chloroform			
BPA−PC	C2	−19.3 (0.7)	−11.3 (2.1)	−8.0	−8.8 (1.2)
	C3	−23.0 (0.3)	−16.2 (2.9)	−6.8	
	C4	−32.8 (1.9)	−16.9 (4.1)	−15.9	
	D2	−13.7 (1.6)	−3.2 (0.6)	−10.5	
	D3	−17.2 (0.8)	−8.1 (1.1)	−9.1	
		DMSO			
	C2	−26.1 (0.5)	−11.3 (2.1)	−14.8	−18.2 (1.0)
	C3	−30.4 (0.4)	−16.2 (2.9)	−14.2	
	C4	−39.1 (0.9)	−16.9 (4.1)	−22.2	
	D2	−20.1 (2.2)	−3.2 (0.6)	−16.9	
	D3	−24.4 (0.5)	−8.1 (1.1)	−16.3	
		propane			
	C2	−11.0 (0.7)	−11.3 (2.1)	0.3	−0.6 (0.6)
	C3	−14.9 (0.3)	−16.2 (2.9)	1.3	
	C4	−23.9 (1.9)	−16.9 (4.1)	−7	
	D2	−5.2 (1.6)	−3.2 (0.6)	−2	
	D3	−9.1 (0.8)	−8.1 (1.1)	−1	

[a] Errors (obtained by block averaging) are given in parentheses.

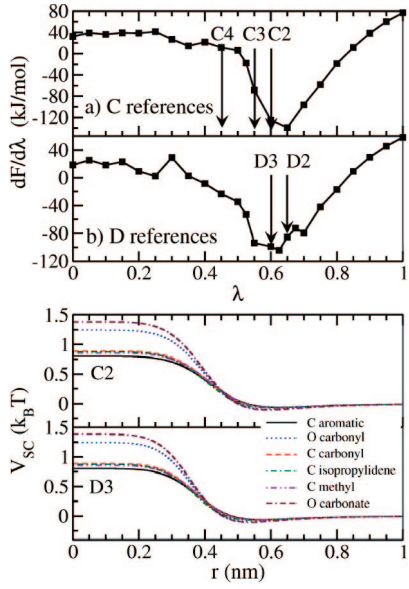

Figure 5. (upper panel) TI curves for the C and D references in BPA−PC with 1 ns equilibration and 1 ns run time. (lower panel) Soft-core potential energy functions $V_{SC}(r,\lambda)$ of the references C2 and D3 with BPA−PC backbone atoms at 480 K.

To resolve this problem, we performed a large number of fast-growth TIs[20] and used exponential averaging of the resulting work distributions to obtain accurate solute free energies in BPA−PC. We have discussed this fast-growth TI approach in greater detail elsewhere.[20] The statistical errors on the free energies obtained from fast-growth TI are 0.6 (propane), 1.0 (DMSO), and 1.2 kJ/mol (chloroform). The fast-growth TI free energies (ΔF^{TI}) are summarized in Table 3 together with the free energies obtained by free energy perturbation (ΔF^{FEP}) based on the various soft cavity reference states.

Figure 5 (upper panel) shows $\partial\Delta F/\partial\lambda$ vs λ for LJ particles C and D (see Table 1) in the BPA−PC microstructure. Note that for $\lambda < 0.5$ the value of $\partial\Delta F/\partial\lambda$ depends on the starting conditions as noted above; i.e., the "hard" particle does not explore the matrix. The choices of the λ values used to define the soft reference states are indicated with the arrows; the corresponding soft-particle potentials for C2 and D3, where only σ differs as a parameter in the potential, are shown in the lower panel. Since BPA−PC contains various atom types, the potentials between soft cores and these atom types are plotted separately. Table 4 summarizes the root-mean-square displacements of C2, C3, C4, D2, D3, and chloroform in the BPA−PC matrix after 1 ns. On this time scale, C2, D2, and D3 move diffusively and explore most of the simulation volume (the box size is 4.87 nm). C3 and C4 only move over distances up to 0.5−0.8 nm, indicating that these reference states are too hard causing the soft particle to stay close to its initial position in the matrix. (The BPA−PC monomer size defined through the carbonate−carbonate distance along the backbone equals 1.1 nm.) On the other hand, chloroform does not move at all on this time scale. This clearly illustrates that the free energy changes obtained by means of (slow-growth) TI using nanosecond simulation times cannot provide reliable results because volume-averaged sampling over the various low-energy minima (cavities) in the matrix is lacking.

Table 4. Root-Mean-Square Displacements (rmsd) in BPA−PC after 1 ns (units of nm)

C2	3.3	D2	7.2
C3	0.8	D3	4.5
C4	0.5	chloroform	0.3

Figure 6 shows the energy distributions $\rho(\Delta U_{REF\rightarrow PROPANE})$ and the reweighted distributions $\rho(\Delta U_{REF\rightarrow PROPANE})\exp[-\beta\Delta U_{REF\rightarrow PROPANE}]$ obtained with the C2 (upper panel) and C4 (lower panel) reference ensembles. The reweighted distribution based on the C2 reference is sampled with reasonable accuracy, unlike the corresponding distribution obtained by sampling the C4 reference state where the distribution is very scattered at the low-energy tail. A similar difference between C2 and C4 emerges with the chloroform and DMSO solutes (not shown). In Figure 7, the running average value of ΔF^{FEP} is shown for chloroform, DMSO, and propane. The lines represent the different soft cavity reference states. Figure 7—interpreted along with the rmsd's in Table 4—clearly illustrates that the C2 and D3 reference states are the optimal ones to achieve statistical convergence and volume averaging on the simulation time scale (10 ns). Although the perturbation free energy based on C3 (Figure 7) converges within 10 ns as well, it is clear from the rmsd in Table 4 that reasonable

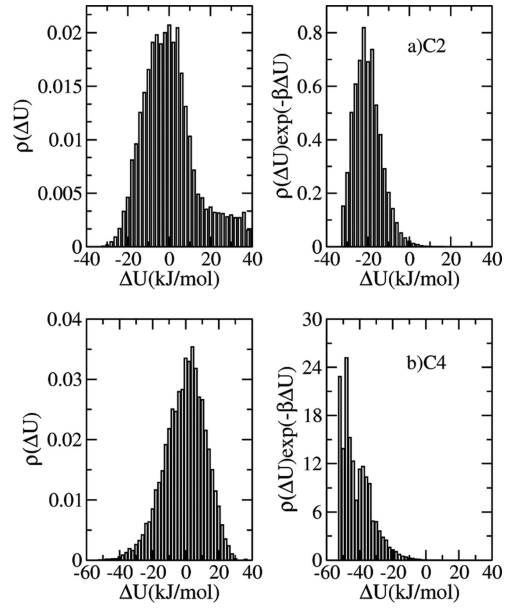

Figure 6. (left) Probability distribution function $\rho(\Delta U)$ and (right) its exponentially weighted distribution $\rho(\Delta U)\exp(-\beta\Delta U)$ corresponding to free energy perturbation of (a) a good reference C2 to propane and (b) a bad reference C4 to propane in BPA−PC.

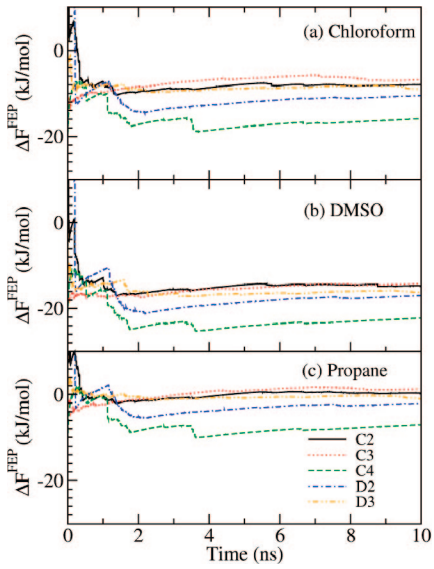

Figure 7. Running average free energy changes of solvation, ΔF^{FEP}, for the solutes (a) chloroform, (b) DMSO, and (c) propane obtained from the perturbation using various reference states (C2, C3, C4, D2, and D3) in BPA−PC.

sampling of the box volume has not been achieved. D2 and, in particular, C4 are not converged (Figure 7), which causes the negative deviation of ΔF^{FEP} in comparison to ΔF^{TI} for D2 and C4 in Table 3. In particular, for the C4 reference (which is too "hard" and does not explore the matrix; see Table 4), the free energy is dominated by a few low-energy ("fortunate") insertions, which are not properly weighted. This corresponds to the scattered, high values in the reweighted energy distribution in the lower panel of Figure 6. For DMSO, with the exception of C4, all reference states systematically predict too positive ΔF^{FEP} values. This result, however, is not surprising for a highly polar solute (the dipole moment of the DMSO model[35] is 5.25 D) treated with a perturbation method based on a reference ensemble of a nonpolar soft cavity. For chloroform and propane, within the error bars of 2−3 kJ/mol, the values of ΔF^{FEP} and ΔF^{TI} are in reasonable agreement for C2, C3, D2, and D3.

We finally point out that the free energy difference $\Delta\Delta F^{\mathrm{FEP}}_{X,Y}$, defined as the difference $\Delta F^{\mathrm{FEP}}_{\mathrm{REF}\rightarrow\mathrm{SOLUTE,X}} - \Delta F^{\mathrm{FEP}}_{\mathrm{REF}\rightarrow\mathrm{SOLUTE,Y}}$, provides the relative solubility of solutes X and Y, i.e., $S_X/S_Y = \exp[-\Delta\Delta F_{X,Y}/RT]$. When applied to chloroform and propane $\Delta\Delta F^{\mathrm{FEP}}_{\mathrm{CHCl_3},\mathrm{C_3H_8}} = -8.3$ kJ/mol (averaged over the C2, C3, D2, and D3 references), which compares to a value of −8.2 kJ/mol obtained by fast-growth TI. For solute pairs involving DMSO, the $\Delta\Delta F^{\mathrm{FEP}}_{\mathrm{DMSO,Y}}$ values are ∼2 kJ/mol more positive than the corresponding value obtained with fast-growth TI. Compared to absolute values, relative solubilities can be calculated with higher accuracy because systematic errors may cancel out in taking the free energy differences. Moreover, uncertainties related to the quality of the force fields become smaller; i.e., effects of a too strong (or weak) solute−matrix nonbonded interaction may largely cancel when comparing, for example, relative solubilities of benzene and toluene.

5. Summary and Conclusions

Molecular simulations are frequently used for calculating solubilities of small gaseous penetrants in polymer microstructures. Unlike for small molecules, solubilities of large-sized penetrants cannot easily be calculated owing to the complexity of the typical free energy surfaces in dense polymer microstructures. Solubilities of large and internally rigid solute molecules are particularly difficult to obtain since these molecules can neither be inserted at once (by Widom test particle insertion) nor be inserted stepwise; in the latter case configurational biasing MC methods[13,14,16] offer advantages with flexible solutes. Because the free energy barriers separating the low-energy minima ("cavities") are typically much larger than k_BT, fully coupled, large molecules are moreover prevented from sampling all possible minima during finite time molecular dynamics simulation, which causes slow-growth thermodynamic (coupling parameter) integration (TI) methods to be computationally inefficient. In this paper, slow-growth TI is used to introduce a Lennard-Jones particle, which is coupled to the matrix up to a value of the coupling parameter where the particle is still sufficiently "soft" to explore all cavity spaces of the matrix. On the basis of this system, a long "soft cavity reference state" trajectory has been generated from which the excess chemical potentials of several solutes have been calculated using a thermodynamic perturbation analysis. This single-step perturbation method[29] offers a useful route to calculating solubilities of bulky additive molecules inside polymeric microstructures, achieving efficient averaging over the microstructure volume on nanosecond time scales.

In this paper the method has been applied to various solutes in liquid octadecane and bisphenol A−polycarbonate (BPA−PC). The excess chemical potentials (free energies) of the solutes propane, chloroform, and dimethyl sulfoxide have been calculated and (for BPA−PC) compared with results obtained by an alternative—equally well applicable—fast-growth thermodynamic integration method.[20] The comparison illustrates excellent agreement for soft cavity references in which the soft-core−matrix atom (repulsive) interaction does not appreciably exceed a value of k_BT. Because a *single* simulation of an appropriate reference state potentially provides information for many different solutes, the method is particularly useful for calculating solubility ratios of large-sized penetrant pairs, which are of comparable size but are chemically different (e.g., toluene/phenol, ethylbenzene/xylene, etc.). We note that the method is not limited to systems with dissolved molecules present at infinite dilution and can be employed at any solute concentration of interest.

Acknowledgment. The authors thank V. A. Harmandaris and V. Marcon for their comments on the manuscript.

References and Notes

(1) Frenkel, D.; Smit, B. *Understanding Molecular Simulation*; Academic Press: New York, 2002.
(2) Widom, B. *J. Chem. Phys.* **1963**, *39*, 2808.
(3) Müller-Plathe, F. *Macromolecules* **1991**, *24*, 6475.
(4) Sok, R. M.; Berendsen, H. J. C.; Van Gunsteren, W. F. *J. Chem. Phys.* **1992**, *96*, 4699.
(5) Gusev, A. A.; Suter, U. W. *J. Chem. Phys.* **1993**, *99*, 2228.
(6) Tamai, Y.; Tanaka, H.; Nakanishi, K. *Macromolecules* **1995**, *28*, 2544.
(7) Van der Vegt, N. F. A.; Briels, W. J.; Wessling, M.; Strathmann, H. *J. Chem. Phys.* **1996**, *105*, 8849.
(8) Cuthbert, T. R.; Wagner, N. J.; Paulaitis, M. E. *Macromolecules* **1997**, *30*, 3058.
(9) Hofmann, D.; Fritz, L.; Ulbrich, J.; Schepers, C.; Bohning, M. *Macromol. Theory Simul.* **2000**, *9*, 293.
(10) Van der Vegt, N. F. A. *J. Membr. Sci.* **2002**, *205*, 125.
(11) Neyertz, S.; Douanne, A.; Brown, D. *J. Membr. Sci.* **2006**, *280*, 517.
(12) Stapleton, M. R.; Panagiotopoulos, A. Z. *J. Chem. Phys.* **1990**, *92*, 1285.
(13) Siepmann, J. I.; Frenkel, D. *Mol. Phys.* **1992**, *75*, 59.
(14) Spyriouni, T.; Economou, I. G.; Theodorou, D. N. *Macromolecules* **1997**, *30*, 4744.
(15) Fukuda, M. *J. Chem. Phys.* **2000**, *112*, 478.
(16) Raptis, V. E.; Economou, I. G.; Theodorou, D. N.; Petrou, J.; Petropoulos, J. H. *Macromolecules* **2004**, *37*, 1102.
(17) Kirkwood, J. G. *J. Chem. Phys.* **1935**, *3*, 300.
(18) Hummer, G. *J. Chem. Phys.* **2001**, *114*, 7330.
(19) Jarzynski, C. *Phys. Rev. Lett.* **1997**, *78*, 2690.
(20) Hess, B.; Peter, C.; Özal, T. A.; Van der Vegt, N. F. A. *Macromolecules* **2008**, *41*, 2283.

(21) Knopp, B.; Suter, U. W. *Macromolecules* **1997**, *30*, 6114.
(22) Van der Vegt, N. F. A.; Briels, W. J. *J. Chem. Phys.* **1998**, *109*, 7578.
(23) Kofke, D. A.; Cummings, P. T. *Mol. Phys.* **1997**, *92*, 973.
(24) Kofke, D. A.; Cummings, P. T. *Fluid Phase Equilib.* **1998**, *41*, 150–151.
(25) Lu, N.; Kofke, D. A. *J. Chem. Phys.* **1999**, *111*, 4414.
(26) Boulougouris, G. C.; Economou, I. G.; Theodorou, D. N. *Mol. Phys.* **1999**, *96*, 905.
(27) Boulougouris, G. C.; Economou, I. G.; Theodorou, D. N. *J. Chem. Phys.* **2001**, *115*, 8231.
(28) Siegert, M. R.; Heuchel, M.; Hofmann, D. *J. Comput. Chem.* **2007**, *28*, 877.
(29) Schafer, H.; Van Gunsteren, W. F.; Mark, A. E. *J. Comput. Chem.* **1999**, *20*, 1604.
(30) Zwanzig, R. W. *J. Chem. Phys.* **1954**, *22*, 1420.
(31) Hahn, O.; Mooney, D. A.; Müller-Plathe, F.; Kremer, K. *J. Chem. Phys.* **1999**, *111*, 6061.
(32) Leon, S.; Van der Vegt, N.; Delle Site, L.; Kremer, K. *Macromolecules* **2005**, *38*, 8078.
(33) Schuler, L. D.; Daura, X.; Van Gunsteren, W. F. *J. Comput. Chem.* **2001**, *22*, 1205.
(34) Tironi, I. G.; Van Gunsteren, W. F. *Mol. Phys.* **1994**, *83*, 381.
(35) Geerke, D. P.; Oostenbrink, C.; Van der Vegt, N. F. A.; Van Gunsteren, W. F. *J. Phys. Chem. B* **2004**, *108*, 1436.
(36) Ryckaert, J.-P.; Ciccotti, G.; Berendsen, H. J. C. *J. Comput. Phys.* **1977**, *23*, 327.
(37) Berendsen, H. J. C.; Postma, J. P. M.; Van Gunsteren, W. F.; DiNola, A.; Haak, J. R. *J. Chem. Phys.* **1984**, *81*, 3684.
(38) Van der Spoel, D.; Lindahl, E.; Hess, B.; Groenhof, G.; Mark, A. E.; Berendsen, H. J. C. *J. Comput. Chem.* **2005**, *26*, 1701.
(39) Chipot, C.; Pohorille, A. Calculating Free Energy Differences Using Perturbation Theory. In Chipot, C., Pohorille, A., Eds.; *Free Energy Calculations—Theory and Applications in Chemistry and Biology*; Springer Series in Chemical Physics No. 86; Springer: Berlin, 2007.

MA702329Q